

Intelligent sequence stratigraphy through a wavelet-based decomposition of well log data

Ali Kadkhodaie^{1,2*} and Reza Rezaee¹.

1. Department of Petroleum Engineering, Curtin University of Technology, Perth, Western Australia

2. Earth Science Department, Faculty of Natural Science, University of Tabriz, Iran

Abstract

Identification of sequence boundaries is an important task in geological characterization of gas reservoirs. In this study, a continuous wavelet transform (CWT) approach is applied to decompose gamma ray and porosity logs into a set of wavelet coefficients at varying scales. A discrete wavelet transform (DWT) is utilized to decompose well logs into smaller frequency bandwidths called Approximations (A) and Details (D).

The methodology is illustrated by using a case study from the Ilam and upper Sarvak formations in the Dezful embayment, southwestern Iran. Different graphical visualization techniques of the continuous wavelet transform results allowed a better understanding of the main sequence boundaries. Using the DWT, maximum flooding surface was successfully recognised from both highest frequency and low frequency contents of signals. There is a sharp peak in all A&D corresponding to the maximum flooding surface (MFS), which can specifically be seen in fifth Approximation (a5), fifth Detail (d5), fourth Detail (d4) and third Detail (d3) coefficients. Sequence boundaries were best recognised from the low frequency contents of signals, especially the fifth Approximation (a5). Normally, the troughs of the fifth Approximation correspond to sequence boundaries where higher porosities developed in the Ilam and upper Sarvak carbonate rocks. Through hybridizing both CWT and DWT coefficient a more effective discrimination of sequence boundaries was achieved.

The results of this study show that wavelet transform is a successful, fast and easy approach for identification of the main sequence boundaries from well log data. There is a good agreement between core derived system tracts and those derived from decomposition of well logs by using the wavelet transform approach.

Keywords: Sequence stratigraphy, continuous wavelet transform, discrete wavelet transform, wavelet packet decomposition, Ilam and upper Sarvak formations, sequence boundaries.

* Corresponding author: Tel/Fax: +618 9266 9366
Email addresses: ali.kadkhodaie@curtin.edu.au & kadkhodaie_ali@tabrizu.ac.ir (Ali Kadkhodaie), r.rezaee@curtin.edu.au (Reza Rezaee)

1. Introduction

Sequence stratigraphy is a branch of geology that attempts to subdivide sedimentary rocks into system tracts based on sequence boundaries. A sequence is defined as a succession of generically related sedimentary strata bounded by unconformities or their correlated correlative conformity (Sloss, 1963). The main sequence boundaries include maximum flooding surface (MFS), transgressive surface (TS), regressive surface (RS) and sequence boundary (SB). Accordingly, there are four system tracts for a complete sequence of sedimentary rocks. Lowstand system tract (LST) forms during sea level fall creating lowstand wedges, slope fans and basin floor fan deposits. Transgressive system tract (TST) includes sediments form as sea level starts to rise and fills incised valleys. TST is characterized by retrogradational parasequence set and onlaps directly onto the sequence boundary. Highstand system tract (HST) is characterized by aggradation and then progradation of parasequences as the rate of sea level rise slows, stops and then reverses. Falling stage system tract (FSST) or forced regression systems tract (FRST) forms as sea level starts to fall and may contain surfaces of forced regression and usually does not contain parasequences. Erosional surfaces and incised valleys form during seal level fall and are known as the basal surface of forced regression (Catuneanu, 2006; Miall, 2010).

In this regard, sequence boundaries are considered as the most significant surfaces. Normally, sequences are derived from seismic data through interpretation of stacking patterns. Macroscopic and microscopic study of core profiles and thin-sections provide major information for discrimination of geological bed boundaries. Such information can then be linked to well logs and seismic data to provide a 3D surface of sequence boundaries in a sedimentary basin.

Application of statistical and intelligent methods has become a key research in sequence stratigraphy . Wavelet transform has recent applications is different disciplines of earth science. The first studies relevant to signal processing and wavelet transform in sequence stratigraphy backs to 2003. Rabiller et al. (2003) used signal processing methods in order to speed up log data interpretations in the framework of sequence stratigraphy and sedimentary bodies' architecture while improving their consistency by minimizing any possible operator bias. Alvarez et al. (2003) characterized lithologic properties of a reservoir using wavelet transform. Their method is based on an estimation of the power energy coefficient of signals corresponding to gamma ray logs as well as seismic traces penetrating the rock. In both cases, they find significant differences in the mean value of the power coefficient. Gersztenkorn et al. (2005) introduced SPICE (Spectral Imaging of Correlative Events) as an attribute that uses the continuous wavelet transform to

1 calculate a bed-form boundary framework from seismic data. They offered a straightforward way to interpret
2 a seismic section similar to the way a geologist in the field maps beds and faults directly from the outcrop. Li
3 et al. (2006) studied on the applicability of the wavelet conversion of gamma ray curve in the sequence
4 stratigraphic subdivision of the Yanchang formation. They obtained different cycle orders through wavelet
5 analysis of gamma ray log. Zhang and Song (2007) utilized the db5 continuous wavelet transform to the GR
6 logging curves and obtained the time-frequency characteristic for further sequence stratigraphic division with
7 multiscale analysis. They concluded that wavelet transform can get over the limitation of manual
8 demarcation by the geologists and present new exploration for the quantitative research of sequence
9 stratigraphy. Pan et al., (2008) identified the stratigraphic formation interfaces through performing wavelet
10 and Fourier transform of gamma ray (GR) and spontaneous potential (SP) logs. Their results from a
11 combination of the wavelet transform and the Fourier transform methods, however, were better than those
12 from the wavelet transform method and the conventional well log analysis. Tokhmechi et al. (2009) applied a
13 combination of wavelet and Fourier transform for identification of fractures from water saturation log. They
14 derived a linear relation between energy of approximated section of water saturation log and fracture density
15 and estimated the number of fractures in each fractured zone. Their method was successfully applied to four
16 wells belonging to one of the Iranian oilfields. Ji et al. (2013) employed gamma ray logs and wavelet
17 transform for high resolution sequence stratigraphic division. Their results show that the division by
18 sequence stratigraphic wavelet transform is more objective and more effective and the division provides a
19 new way to high-resolution sequence stratigraphy.

20 The current research reaps the benefits of both continuous wavelet transform (CWT) and discrete wavelet
21 transform (DWT) to perform a sequence stratigraphic division based on a combination of petrophysical well
22 logs in the Ilam and upper Sarvak formations, Dezful embayment. It is worth mentioning that the main
23 elements of this research are based on other researchers' work, which is not novel in their own rights. For
24 example, CWT and DWT or well logs interpretation are well-known technique, however, the integrated
25 approach presented in this study aids in easier and more effective determination of sequence boundaries.
26 Actually, the results obtained in this study support the conventional methods of sequence boundaries
27 determination through looking at well log signatures. The subtle changes in well log responses associated
28 with sequence boundaries can be highlighted through wavelet coefficients.

29 **2. Geological setting**

1 The Zagros fold and thrust belt (Zagros FTB) is an approximately 1800 km long zone of deformed crustal
2 rocks, formed in the foreland of the collision between the Arabian Plate and the Eurasian Plate. It hosts one
3 of the world's largest petroleum provinces, containing about 49% of the hydrocarbon reserves in fold and
4 thrust belts and about 7% of all reserves globally (Sephehr and Cosgrove, 2004; Copper, 2007).
5

6 The study area is located between the southern part of the Zagros fold-trust belt and the northern part of the
7 Dezful embayment (Fig. 1). During the late Mesozoic and early Cenozoic era many prolific onshore source
8 rocks (such as Kazhdumi, Gurpi and Pabdeh formations) and reservoir units (e.g. Asmari, Ilam and Sarvak
9 formations) developed in the study area. During the Miocene this area became a depocentre, in which locally
10 thick Gachsaran evaporite cap rock was deposited. The presence of locally thick Gachsaran salt has caused
11 disharmonic folding between the upper and lower sequences (McQuarie, 2004; Sherkati et al., 2005). Khami
12 and Bangestan groups are the main geological units over the Dezful embayment. The Khami group consists
13 of Fahliyan, Gadvan and Dariyan. Bangestan group, which is the target of the current study, includes the
14 main reservoir units of Ilam and Sarvak formations over the area.
15

16 The Upper Cretaceous Ilam Formation consists of chalky to granular, porous, partly dolomitized, limestones.
17 Particularly the formation contains a very porous interval of limestone in the middle part with very high
18 saturation.
19

20 The Middle Cretaceous Sarvak Formation is comprised of a thick sequence of white chalky mudstone and
21 light-brown compact mudstone-wackestone. The uppermost part of the Sarvak Formation consists of red-
22 brown and grey-green shale considered as "Laffan" shale member. The stratigraphic column of the study area
23 is shown in Fig. 2.
24

25 **3. Methodology: continuous and discrete wavelet transform**

26 Wavelet transform is a signal processing tool that converts a signal to a different form. Such a conversion
27 can reveal the hidden information in signal which can in turn be used in geological interpretations. The signal
28 in this case study is a set of well logging data including gamma ray and porosity logs including neutron and
29 sonic logs measured at drilling wells. CWT and DWT are two main types of wavelet transform which can be
30 used in 1D, 2D (image analysis) and 3D wavelet transform applications.
31

32 **The continuous wavelet transform** measures the similarity between a signal and a wavelet Ψ as an
33 analyzing function. The CWT compares the signal to shifted and compressed or stretched versions of a
34 wavelet. Stretching or compressing a wavelet is referred to as dilation or scaling. By comparing the signal to
35

the wavelet at various scales (α) and positions (β), a function of two variables is obtained. The CWT is calculated as follows (Chang et al., 2000a, b).

$$C(\alpha, \beta, f(t), \Psi(t)) = \int_{-\infty}^{\infty} f(t) \cdot \frac{1}{\sqrt{\alpha}} \Psi * \left(\frac{t-\beta}{\alpha} \right) dt \quad (\text{Eq. 1})$$

Where α is scale parameter ($\alpha > 0$), β is position parameter, $f(t)$ is signal and $\Psi(t)$ is analyzing wavelet. In addition to scale and position parameters, the choice of wavelet also affects the results of CWT coefficients. A flow chart of the computational algorithm of CWT is illustrated in Fig. 3a. It is worth mentioning that correlation (C) between the wavelet and the chosen section of the signal is calculated by using an inner product. In the case of higher similarity between signal energy and wavelet energy parameter C may be interpreted as correlation coefficient. Normally, the wavelet energy and signal energy does not equal and hence CWT coefficients are not directly interpreted as correlation coefficient (Matlab user's guide, 2015).

The discrete wavelet transform (DWT) implements the wavelet transform by using a discrete set of the wavelet scales and translations following some defined rules. Such a transform decomposes the signal into set of mutually orthogonal wavelets, which is the main difference from the CWT. The main advantage of decomposition is its ability of deconstructing complex signals into basis signals of finite bandwidth, and then reconstructing them again with very little loss of information. Also, decomposition can be used for denoising of the signal. Using wavelet we can suppress noise which are out of frequency band of the signal.

In DWT, the wavelet can be constructed from a scaling function that should be orthogonal to its discrete translations.

$$\Psi(t) = \sum_{k=-\infty}^{\infty} a_k \Psi(S_t - k) \quad (\text{Eq. 2})$$

where S is a scaling factor (usually taken as 2). Usually only few of the coefficients a_k are nonzero which simplifies the calculations. Moreover, the area between the function must be normalized and scaling function must be orthogonal to its integer translates.

There are several types of implementation of the DWT algorithm. In the most known algorithm, two sets of coefficients are computed including Approximations (A) and Details (D) though applying two filters. A low-pass h_0 filter for Approximations and a high-pass h_1 filter for Details followed by dyadic decimation (Mallat, 1989; Daubechies, 1992; Meyer, 1990). The result of DWT algorithm is an array of the same length as the input signal, where the data are usually sorted from the largest scales to the smallest ones. The algorithm of DWT is graphically illustrated in Fig. 3b.

4. Relationship between well logs and sequence boundaries

1
2 There are different sources of information for identification of boundaries of sedimentary sequence in a
3 series of rock units. Sequence boundaries can be identified from petrographic studies of thin-section
4 photomicrographs, well logging data and seismic profiles. Normally, the integration of the mentioned
5 sources of information will results it a more accurate discrimination of sequence boundaries. However, such
6 studies suffer from core data scarcity, incomplete well logging data or lack of seismic profiles or their poor
7 quality. Core data represent real rock properties but not available for all drilled wells or for the whole
8 intervals of a cored-well. Normally, well logs are available in all wells of a hydrocarbon field. They can
9 serve as a main source of information for sequence stratigraphic studies specially when combined with core
10 data.
11

12 Main boundaries of a sedimentary sequence are sequence boundary (SB), regressive surface (RS),
13 transgressive surface (TS) and maximum flooding surface (MFS). Usually, there is a good correlation
14 between well log responses and sequence boundaries. By definition, MFS is a surface of deposition at the
15 time the shoreline is at its maximum landward position (i.e. the time of maximum transgression)
16 (Posamentier and Allen, 1999). At the time of maximum movement of shoreline towards land many fine
17 grained sediments such as clays and shale are precipitated. Due to the presence of radioactive and often
18 organic rich shale and clays MFS is represented by a higher gamma ray log reading including CGR
19 (corrected gamma ray) or SGR (sum gamma ray) and hence higher volume of shale. Higher clay content
20 causes high reading is neutron porosity log and sonic transit time, while density log reading decreases due to
21 lower density of clay minerals in comparison to other constituents of sandstones and carbonate rocks such as
22 quartz, feldspar, calcite and dolomite. Accordingly, in a reservoir unit MFS correspond to a higher GR
23 (gamma ray), a higher NPHI (SNP, sidewall neutron porosity & CNL, compensated neutron porosity), a
24 higher DT (BHC, borehole compensated sonic log) and a lower RHOB (FDC, formation density
25 compensated) log readings. Accordingly it is expected to correlate maximum occurrence of shaly intervals
26 with maximum flooding surface while high porosity clay free limestone and dolomitic intervals correspond
27 to sequence boundaries. Shale show a higher porosity and a lower density readings. Clay bound water causes
28 an increase in neutron log readings as its tool is sensitive to hydrogen atom in any form present in the
29 formation. Moreover, clay minerals increase sonic log reading due to their lower density and water available
30 in their pores and structure causing slowness velocity.
31
32
33
34
35
36
37
38
39
40
41
42
43
44
45
46
47
48
49
50
51
52
53
54
55
56
57
58
59
60
61
62
63
64
65

1
2
3
4
5
6
7
8
9
10
11
12
13
14
15
16
17
18
19
20
21
22
23
24
25
26
27
28
29
30
31
32
33
34
35
36
37
38
39
40
41
42
43
44
45
46
47
48
49
50
51
52
53
54
55
56
57
58
59
60
61
62
63
64
65

Sequence boundaries (SB) envelope sequences that are identified as significant erosional unconformities or their correlative conformities. These boundaries are the result of a fall in sea level that erodes the sub-aerially exposed sediment surface of the earlier sequence or sequences. These boundaries are diachronous, capping the previous highstand systems tract and eroding the surface of the downstepping sediments deposited during accompanying forced regression associated with the sea level fall (Catuneanu, 2002). A sequence boundary is a high porosity area, which is characterized by lower gamma ray, higher neutron porosity after shale effect correction, higher sonic transition time and lower density log readings. Accordingly, sequence boundaries are in connection to the peaks of porosity logs after shale correction has been considered (low gamma ray porous zones). Because shaly intervals contain bound water, which is mistakenly interpreted as porosity in neutron logs.

5. Application to the Ilam and Sarvak formations

There are many different admissible wavelets that can be chosen in the CWT. The major wavelet family names are Haar (haar), Daubechies (db), Symlets (sym), Coiflets (coif), Biorthogonal (bior), ribo (Reverse biorthogonal wavelets) and discrete approximation of Meyer wavelet (dmey). Wavelets are chosen based on the signal features subjected to detection purpose. In this research, as matching pursuit algorithm is used for selection of the most appropriate wavelet for signal processing. Matching pursuit is a greedy algorithm that computes the best nonlinear approximation to a signal in a complete, redundant dictionary. Matching pursuit was used to recover signal through building a sequence of sparse approximations to the signal stepwise. For this purpose, different wavelets were used for recovering signal. Examining different wavelets revealed that db wavelet is associated with the lowest mean squared error in signal approximation. Accordingly, a db-5 wavelet was used for continuous and discrete wavelet analysis of well logging data. As mentioned earlier, signal is here referred to as gamma ray and porosity logs used for sequence strigraphy analysis.

In continue, the Wavelet Packet analysis method was employed to decompose signal into eight frequency levels. One step in the wavelet transform calculates a low pass (scaling function) result and a high pass (wavelet function) result. The low pass result is a smoother version of the original signal. The low pass result recursively becomes the input to the next wavelet step, which calculates another low and high pass result, until only a single low pass result is calculated. The wavelet transform applies the wavelet transform step to the low pass result. The Wavelet Packet transform applies the transform step to both the low pass and the high pass result. Actually, the wavelet packet transform can be viewed as a tree. The root of the tree is the original data set. The next level of the tree is the result of one step of the wavelet transform. Subsequent

1 levels in the tree are constructed by recursively applying the wavelet transform step to the low and high pass
2 filter results of the previous wavelet transform step. Wavelet Packets provided a computationally-efficient
3 alternative with sufficient frequency resolution (Fig. 4). As seen, the majority of the signal (here gamma ray
4 log) energy belongs to low frequency bounds (1-62.5 Hz). That is, the low frequency band of signals are in
5 better agreement with the signal energy and can effectively be used for sequence boundaries discrimination.
6
7

8
9 By using the CWT thirty two coefficients (corresponding to scale 1 through 32) were obtained, which are
10 shown as example for GR log in Fig. 5. A gray scale coloration mode, which is provided a good resolution,
11 is chosen for representation of wavelet coefficients of GR log.
12
13

14 Applying DWT with the db-5 wavelet the well logs have been decomposed into five approximation and five
15 details (Fig. 6). As shown in Fig. 6, red curve represents signal (here GR log), blue curve shows the fifth
16 approximation and details 1 through 5 are displayed by green color. The signal can be constructed from the
17 summation of fifth approximation (a5) and all details ($GR=d1+d2d3+d4+d5+a5$). As seen, not only the sharp
18 peaks but also the weak fluctuations of GR log have remarkably been fortified though application of DWT.
19
20
21
22
23
24
25
26
27
28
29
30
31
32
33
34
35
36
37
38
39
40
41
42
43
44
45
46
47
48
49
50
51
52
53
54
55
56
57
58
59
60
61
62
63
64
65

6. Results and discussion

The main sequence boundaries and corresponding system tracts identified for the Ilam and Upper Sarvak formations are graphically illustrated in Fig. 7. The results of applying continuous wavelet transform on GR, NPHI and DT logs for the reservoir intervals are displayed in Fig. 8. The CWT coefficients are displayed at all integer scales from 1 to 32 in a grey scale representation on a scalogram. The low scale CWT coefficients (towards 1) correspond to the fine-scale features in the signal vector. High scale values (towards 32) stretch the wavelet and correlate better with the low frequency content of the signal. The high scale CWT coefficients represent the coarse-scale features in the input signal from well logs. As seen in Fig. 8, CWT has been successful in highlighting the main sequence boundaries from gamma ray and porosity logs. There is a good agreement between maximum flooding surface and wavelet coefficients. The colour representation of the continuous wavelet transform coefficients from scales 1 to 32 created a cone-shaped features in the scalogram of Fig. 8 corresponding to MFS. MFS is often characterized by higher gamma ray peaks due to the presence of radioactive and often organic-rich shale, Glauconite and carbonate hardgrounds. Often in a landward direction the MFS may match the underlying TS formed during or just after the initial transgressive phase that immediately follow sea level lowstands.

Normally, a sequence boundary is formed as response of sea level fall corresponding to unconformities or their correlative conformities. As mentioned earlier, it is usually associated with lower gamma ray, higher neutron porosity, higher sonic transition time and lower density log readings (low clay porous zones). In this study, sequence boundaries correspond to the peak of porous zone, which is characterized by subtle light colours on the scalogram. The identified sequence boundaries are of type 2 characterized by subaerial exposure and a downward shift in onlap landward of the depositional shoreline break (usually at base level or at sea level). Overlying beds onlap this surface. However, care must be taken when relating high porosity peaks of well logs to sequence boundaries as some fraction of the higher porosity is attributed to the action of the diagenetic processes such as fracturing, dissolution and recrystallization. Such sequence boundaries lack subaerial erosion associated with the down-cutting of streams and lack a basin-ward shift in facies. They probably form when the rate of sea-level fall is less than the rate of subsidence at the depositional shoreline break. The lack of a basin-ward shift in facies and the lack of a relative fall in sea level at the depositional shoreline break means that there are essentially no criteria by which to recognize a type 2 sequence boundary in outcrop.

1 The results of DWT are shown as coloured curves on the right side of Fig. 9. As mentioned earlier, a db-5
2 wavelet was applied to decompose GR, NPHI and DT logs in to five Approximations and five Details by
3 using continuous wavelet transform. In order to avoid a busy plot, only the results of GR log decomposition
4 are displayed. Red curves represent NPHI, DT and GR logs, respectively. Fifth approximation (a5) is shown
5 by green colour and d1 through d5 are displayed by cyan, black, blue and magenta colours, respectively. As
6 is seen in Fig. 9, maximum flooding surface is successfully recognised from both highest frequency and low
7 frequency contents of signal (here GR log). There is a sharp peak in all A&D corresponding to MFS, which
8 can clearly be seen in a5, d5, d4 and d3 coefficients. Sequence boundaries are best recognised from the low
9 frequency contents of signals specially the Fifth Approximation (a5). Normally, the troughs of fifth
10 Approximation correspond to sequence boundaries where higher porosities developed in the Ilam and upper
11 Sarvak carbonate rocks.

12 On the right side of Fig. 9 image plot of the CWT coefficient, main system tracts along with lithology and
13 fluids column of the Ilam and upper Sarvak formation are illustrated. Volumetric mineralogy has been
14 derived from well log data by solving multi-mineral equations with graphic well log and core controls.
15 Comparing the results of CWT and DWT it could be concluded that a better discrimination of sequence
16 boundaries and their corresponding systems tracts has been achieved. There is a good agreement between
17 CWT and DWT results the extracted coefficient support Approximations and Details. The peaks seen in
18 original well logs at sequence boundaries becomes sharper and clearer by using the wavelet decomposition
19 approach.

20 Actually, each individual log can be used for recognition of sequence boundaries however; logging data are
21 associated with uncertainties and any abnormal peak can be misinterpreted as a specific type of sequence
22 boundary. That is why using a set of well logging data which are sensitive to sequence boundaries variation
23 is recommended. DWT can reveal MFS boundaries in situations that the conventional approaches will fail. In
24 the meantime, SB correspond to the peak of porous zone which is characterized by subtle light colours on the
25 CWT scalogram.

26 Considering the both wavelet transform approaches four third order sequences are determined for the Ilam
27 Formation. In a similar way, the upper Sarvak Formation is divided into two third order sequences. The main
28 system tracts observed in the Ilam and Sarvak formations are transgressive system tract (TST) and highstand
29 system tract (HST) where good reservoir quality rocks with a considerable amount of porosity and
30 hydrocarbon saturation are developed. Falling stage system track (FSST) was not observed in the carbonate

1 sequences of the studied formations due to rapid sea level fall which is usually associated with no or starve
2 sedimentation. Normally, FSST is associated with basin floor/ slope fans, while lowstand system (LST) track
3 forms lowstand wedges.
4

5 Finally, it is tried to determine sequence boundaries by hybridizing both CWT and DWT coefficients.
6 Through stacking continuous and discrete wavelet coefficients an step is made towards more effective
7 discrimination of sequence boundaries. After stacking a single wavelet coefficient log is obtained for each of
8 the CWT and DWT results. The stacked coefficients were normalized be comparable to each other. The final
9 input to wavelet transform was obtained by multiplying normalized stacked coefficients of both continuous
10 and discrete wavelet transforms. Coefficients multiplication approach strengthens sequence boundaries
11 discrimination by creating a product log from CWT-DWT results. The product log which will in turn be fed
12 to a subsequent wavelet transform. A cross-section showing the correlation of the systems tracts derived
13 based on hybridized CWT-DWT wavelet coefficients in three wells of the study area is shown in Fig. 10. As
14 is seen there is a good agreement between determined sequence boundaries by using the hybrid wavelet
15 methods.
16
17
18
19
20
21
22
23
24
25
26
27
28
29
30

31 **7. Conclusions**

32 Wavelet transform is a useful way to highlight the sequence boundaries through decomposition of well logs
33 data into a set of coefficients. Through converting wavelet coefficients into image and using an appropriate
34 coloration mode a better interpretation of sequence boundaries is achieved.
35
36

37 Continuous wavelet transform of gamma ray, neutron and sonic logs is found successful in highlighting
38 maximum flooding surfaces. The low scale CWT coefficients (towards 1) correspond to the fine-scale
39 features in the signal vector. High scale values (towards 32) stretch the wavelet and correlate better with the
40 low frequency content of the signal. The high scale CWT coefficients represent the coarse-scale features in
41 the input signal from well logs.
42
43
44
45
46
47
48
49

50 Using the DWT, maximum flooding surface is successfully recognised from the both highest frequency and
51 low frequency contents of signals. There is a sharp peak in all A&D corresponding to MFS which can
52 specifically be seen in a5, d5, d4 and d3 coefficients.
53
54

55 Sequence boundaries are best recognised from the low frequency contents of signals especially the fifth
56 Approximation (a5). Normally, the troughs of the fifth Approximation correspond to sequence boundaries
57 where higher neutron porosities developed in the Ilam and upper Sarvak carbonate rocks.
58
59
60
61
62
63
64
65

1
2 As the results show, not only the sharp peaks but also the weak fluctuations of GR log have remarkably been
3 fortified through application of DWT.

4
5 Hybridizing the CWT and DWT coefficients strengthens key signatures of well logs corresponding to
6
7 sequence boundaries. Implementation of wavelet transform on the product of stacked coefficients leads to a
8
9 successful determination of system tracts. It is expected to use hybrid wavelet decomposition approach as an
10
11 instrumental and effective way to create sharper and clearer peaks at sequence boundaries from original well
12
13 log data.
14
15
16
17
18
19
20
21
22
23
24
25
26
27
28
29
30
31
32
33
34
35
36
37
38
39
40
41
42
43
44
45
46
47
48
49
50
51
52
53
54
55
56
57
58
59
60
61
62
63
64
65

8. Nomenclature

1
2
3 a_k : Coefficients of the discrete wavelet transform

4
5 A: Approximations of discrete wavelet transform

6
7 a_i : i^{th} approximation of discrete wavelet transform

8
9 a_n is the scalar weighting factor (amplitude) for the atom in matching pursuit algorithm

10
11 α : Scale parameter in wavelet transform

12
13 β : Position parameter in wavelet transform

14
15 BHC: Borehole compensated sonic log

16
17 bior: Biorthogonal wavelets

18
19 C: Correlation between wavelet and chosen section of signal

20
21 CGR: Uranium corrected gamma ray

22
23 CNP: Compensated neutron log

24
25 coif: Coiflets wavelet

26
27 CWT: Continuous wavelet transform

28
29 D: Details of discrete wavelet transform

30
31 d_i : i^{th} detail of discrete wavelet transform

32
33 db: Daubechies wavelet

34
35 dmey: Discrete approximation of Meyer wavelet

36
37 DT: Sonic transit time log

38
39 DWT: Discrete wavelet transform

40
41 FDC: formation density compensated

42
43 FSST: Falling stage system tracts

44
45 FRST: Forced regression systems tract

46
47 $f(t)$: Signal

48
49 GR: Gamma ray log

50
51 g_m : atoms in mating pursuit algorithm

52
53 H : Hilbert space in matching pursuit algorithm

54
55 h_0 : Low-pass frequency filter

56
57 h_1 : High-pass frequency filter

1 haar: Haar wavelet
2 HST: Highstand system tract
3
4 LST: Lowstand system tract
5
6 mexh: Mexican hat wavelet
7
8 MFS: Maximum flooding surface
9
10 MSE: Mean squared error
11
12 NPFI: Neutron log porosity
13
14 ribo: Reverse biorthogonal wavelets
15
16 RHOB: Density log
17
18 R_N : Residual in matching pursuit algorithm
19
20
21 RS: Regressive surface
22
23 S: Scaling factor in discrete wavelet transform
24
25 SB: Sequence boundary
26
27 SGR: Sum Gamma Ray
28
29 SNP: Side-wall neutron porosity
30
31 SP: Spontaneous potential
32
33 sym: Symlets wavelet
34
35 TS: Transgressive surface
36
37 TST: Transgressive system tract
38
39 (t): Analysing wavelet
40
41 ZFTB: The Zagros fold and thrust belt
42
43
44
45
46
47
48
49
50
51
52
53
54
55
56
57
58
59
60
61
62
63
64
65

Appendix 1: Matching Pursuit

Matching pursuit (MP) is a sparse approximation algorithm which involves finding the "best matching" projections of multidimensional data onto the span of an over-complete (i.e., redundant) dictionary D . The basic idea is to approximately represent a signal f from Hilbert Space H as a weighted sum of finitely many functions g_m (atoms) taken from D . An approximation with N atoms has the form (Mallat and Zhang, 1993)

$$f(t) \approx \hat{f}_N(t) := \sum_{n=1}^N a_n g_{\gamma_n}(t)$$

where a_n is the scalar weighting factor (amplitude) for the atom $g_{\gamma_n} \in D$. Normally, not every atom in D will be used in the sum. Instead, matching pursuit chooses the atoms one at a time in order to maximally (greedily) reduce the approximation error. This is achieved by finding the atom that has the biggest inner product with the signal (assuming the atoms are normalized), subtracting from the signal an approximation that uses only that one atom, and repeating the process until the signal is satisfactorily decomposed, i.e., the norm of the residual is small.

The residual after calculating γ_n and a_n is denoted by

$$R_{N+1} = f - \hat{f}_N$$

If R_N converges quickly to zero, then only a few atoms are needed to get a good approximation to f . Such sparse representations are desirable for signal coding and compression. More precisely, the sparsity problem that matching pursuit is intended to approximately solve is

$$\min_x \|f - Dx\|_2^2 \text{ subject to } \|x\|_0 \leq N,$$

where $\|x\|_0$ and L_0 pseudo-norm (i.e. the number of nonzero elements of x). In the previous notation, the nonzero entries of x are $x_{\gamma_n} = a_n$ and the x_{γ_n} th column of matrix D is g_{γ_n} .

The algorithm iteratively generates for any signal f and any dictionary D a sorted list of atom indices and weighting scalars which represent the sub-optimal solution to the problem of sparse signal representation.

Matching Pursuit Algorithm:

Input: Signal $f(t)$, Dictionary D .

Output: List of coefficients $(a_n)_{n=1}^N$ and indices for corresponding atoms $(\gamma_n)_{n=1}^N$.

Initialization:

$R_1 \leftarrow f(t)$;

$n \leftarrow 1$;

Repeat:

Find $g_m \in D$ with maximum inner product $|\langle R_n, g_m \rangle|$;

$a_n \leftarrow \langle R_n, g_m \rangle / \|g_m\|^2$;

$R_{n+1} \leftarrow R_n - a_n g_m$;

$n \leftarrow n + 1$

Until stop condition (for example: $\|R_n\| < \text{threshold}$)

- "." is a shorthand for "changes to". For instance, " $largest \leftarrow item$ " means that the value of $largest$ changes to the value of $item$.
- "**return**" terminates the algorithm and outputs the value that follows.

References

- 1
2 Alvarez, G., Sanso, B., Michelena, R.J., Jimenez, J.R., 2003. Lithologic characterization of a reservoir using
3 continuous wavelet transform. *IEEE Transactions on Geoscience and Remote Sensing* 41 (1), 59–65.
4
5 Catuneanu, O., 2002. Sequence stratigraphy of clastic systems: concepts, merits, and pitfalls, *Journal of*
6
7 *African Earth Sciences* 35 (1), 1-43.
8
9 Catuneanu, O., 2006. *Principles of Sequence Stratigraphy*. Elsevier B.V., UK. 375p.
10
11 Chanh, S.G., Yu, B., Vetterli, M., 2000a. Spatially adaptive wavelet thresholding based on connect
12
13 modelling for image de-noising. *IEEE transactions on Image Processing* 9, 1522-1531.
14
15 Chanh, S.G., Yu, B., Vetterli, M., 2000b. Adaptive wavelet thresholding for image de-noising and
16
17 compression. *IEEE transactions on Image Processing* 9, 1532-1546.
18
19 Cooper, M. 2007. "Structural style and hydrocarbon prospectivity in fold and thrust belts: a global review".
20
21 In Gersztenkorn, A., Smythe, J., Radovich, B., 2005. Stratigraphic detail from wavelet based spectral
22
23 imaging. *Canadian Society of Exploration Geophysics (CSEG)* 30 (4), 1-10.
24
25 Ries A.C., Butler R.W. & Graham R.H. Deformation of the Continental Crust: The Legacy of Mike Coward.
26
27 *Special Publications 272*. London: Geological Society. pp. 447–472. ISBN 978-1-86239-215-1.
28
29 Daubechies, I., 1992. Ten lectures on wavelets, CBMS-NSF conference series in applied mathematics.
30
31 Society for Industrial and Applied Mathematics. 357p.
32
33 Ji, D.W., Li, J., Lu, G.D., 2013. Application of Wavelet Transform in High-Resolution Sequence
34
35 Stratigraphic Division. *Advanced Materials Research* 772, 823-827.
36
37 Li, X-B., Gou, Y-R., Liu, H-Q., 2006. The Application of Wavelet Analysis in Sequence Stratigraphic
38
39 Subdivision of the Yanchang Formation, Ordos Basin [J]. *Natural Gas Geoscience* 17(6), 779-782.
40
41 McQuarrie, N. 2004. Crustal scale geometry of the Zagros fold–thrust belt, Iran. *Journal of Structural*
42
43 *Geology (Elsevier)* 26 (3): 519–535.
44
45 Mallat, S., 1989. A theory for multiresolution signal decomposition: the wavelet representation," *IEEE*
46
47 *Pattern Anal. and Machine Intell.* 11 (7), 674-693.
48
49 Mallat, S.G., Zhang, Z., 1993. Matching Pursuits with Time-Frequency Dictionaries, *IEEE Transactions on*
50
51 *Signal Processing*, December, pp. 3397–3415
52
53 Matlab user's guide, 2015. Wavelet transform toolbox. The Mathworks Inc.
54
55 Meyer, Y., 1990. *Ondelettes et opérateurs*, Tome 1, Hermann Ed., 215p (English translation: *Wavelets and*
56
57 *operators*, Cambridge Univ. Press. 1993.)
58
59
60
61
62
63
64
65

- 1 Miall, A., 2010. *The Geology of Stratigraphic Sequences*. Springer, Berlin Heidelberg, 522p.
- 2 Pan, S-Y., Hsieh, B-S., Lu, M-T., Lin, Z-S., 2008. Identification of stratigraphic formation interfaces using
3 wavelet and Fourier transforms. *Computers & Geosciences* 34, 77–92
- 4
5 Posamentier, H.W., Allen, G.P., 1999. *Siliciclastic Sequence Stratigraphy: concepts and applications*.
6
7 *SEPM Concepts in Sedimentology and Paleontology* 7, 210p.
- 8
9 Rabiller, P.J.Y.M., Robail, F., Remacha, E., Richard, L., Sancho-Jaquel, F-J., Climent, F., Fernandez, L.P.,
10
11 2003. Sequence stratigraphy applied to log interpretation: improving methodology by means of signal
12
13 processing techniques and outcrop calibration. AAPG International Conference, Barcelona, Spain,
14
15 September 21-24, pp. 1-5.
- 16
17 Sepehr, M., Cosgrove, J.W. 2004. Structural framework of the Zagros Fold-Trust Belt, Iran. *Marine and*
18
19 *Petroleum Geology* 21, 829-843.
- 20
21 Sherkati, S., Molinaro, M., de Lamotte, D. Frizon., Letouzey, J., 2005. Detachment folding in the Central and
22
23 Eastern Zagros fold-belt (Iran): salt mobility, multiple detachments and late basement control. *Journal of*
24
25 *Structural Geology Elsevier* 27 (9), 1680–1696.
- 26
27 Sloss, L.L., 1963. Sequences in the Cratonic Interior of North America." *Geological Society of America*
28
29 *Bulletin*. 74, 93-114.
- 30
31 Tokhmechi, B., Memarian, H., Rasouli, V., Ahmadi Noubari, H., Moshiri, B., 2009. Fracture detection from
32
33 water saturation log data using a Fourier–wavelet approach. *Journal of Petroleum Science and Engineering*
34
35 69, 129-138.
- 36
37 Zhang, J., Song, A., 2010. Application of Wavelet Analysis in Sequence Stratigraphic Division of Glutenite
38
39 Sediments. *International Conference on Challenges in Environmental Science and Computer Engineering*,
40
41 IEEE, pp. 204-207
- 42
43
44
45
46
47
48
49
50
51
52
53
54
55
56
57
58
59
60
61
62
63
64
65

Figure captions

Figure 1. Location map of study area between southern part of the Zagros fold-thrust belt and northern part of the Dezful embayment (Copper, 2007). Location map of the studied wells A, B and C is shown on the map by filled red circles.

Figure 2. Stratigraphic column of the study area. Ilam and Sarvak are the major oil bearing reservoirs.

Figure 3. Graphical illustration of continuous wavelet transform algorithm (a). Schematic diagram showing computational algorithm of discrete wavelet transform (b)

Figure 4. Wavelet packets decomposition of signal into eight frequency bands. As shown, majority of the signal (here gamma ray log) energy belongs low frequency bounds (1-62.5 Hz).

Figure 5. An image representation of CWT coefficients. CWT coefficients were obtained at 32 scales by using db-5 wavelet and a grey scale coloration mode is chosen for representation of the results.

Figure 6. Applying DWT with the db-5 wavelet decomposes well logs into five approximation and five details. As is seen gamma ray is reconstructed from summation of d1, d2, d3, d4, d5 and a5.

Figure 7. Main sequence stratigraphic units of Ilam and upper Sarvak formation in the study area

Figure 8. The results of applying continuous wavelet transform on GR, NPHI and DT logs along with lithology and fluids column for the Ilam and upper Sarvak formations. There is a good agreement between maximum flooding surface and wavelet coefficients. The color representation of the continuous wavelet transform coefficients from scales 1 to 32 created a cone shaped features in the scalogram corresponding to MFS. Sequence boundaries correspond to the peak of porous zone which is characterized by subtle light colors on the scalogram.

Figure 9. The results of applying DWT on GR, NPHI and DT logs along with lithology and fluids column for the Ilam and Upper Sarvak formations. Maximum flooding surface is successfully recognized from the both highest frequency and low frequency contents of signal (here GR log). There is a sharp peak in all A&D corresponding to MFS which can clearly be seen in a5, d5, d4 and d3 coefficients. Sequence boundaries are best recognized from the low frequency contents of signals specially the fifth Approximation (a5). Normally, the troughs of fifth Approximation correspond to sequence boundaries where higher porosities developed.

Figure 10. Cross-section showing the correlation of the systems tracts derived based on hybrid CWT-DWT wavelet coefficients in three wells of the study area. For this purpose, first continuous and discrete wavelet coefficients were stacked and normalized individually. Afterward both CWT and DWT were applied on the

product of stacked coefficients. As is seen there is a good agreement between determined sequence boundaries by using the hybrid wavelet methods.

1
2
3
4
5
6
7
8
9
10
11
12
13
14
15
16
17
18
19
20
21
22
23
24
25
26
27
28
29
30
31
32
33
34
35
36
37
38
39
40
41
42
43
44
45
46
47
48
49
50
51
52
53
54
55
56
57
58
59
60
61
62
63
64
65

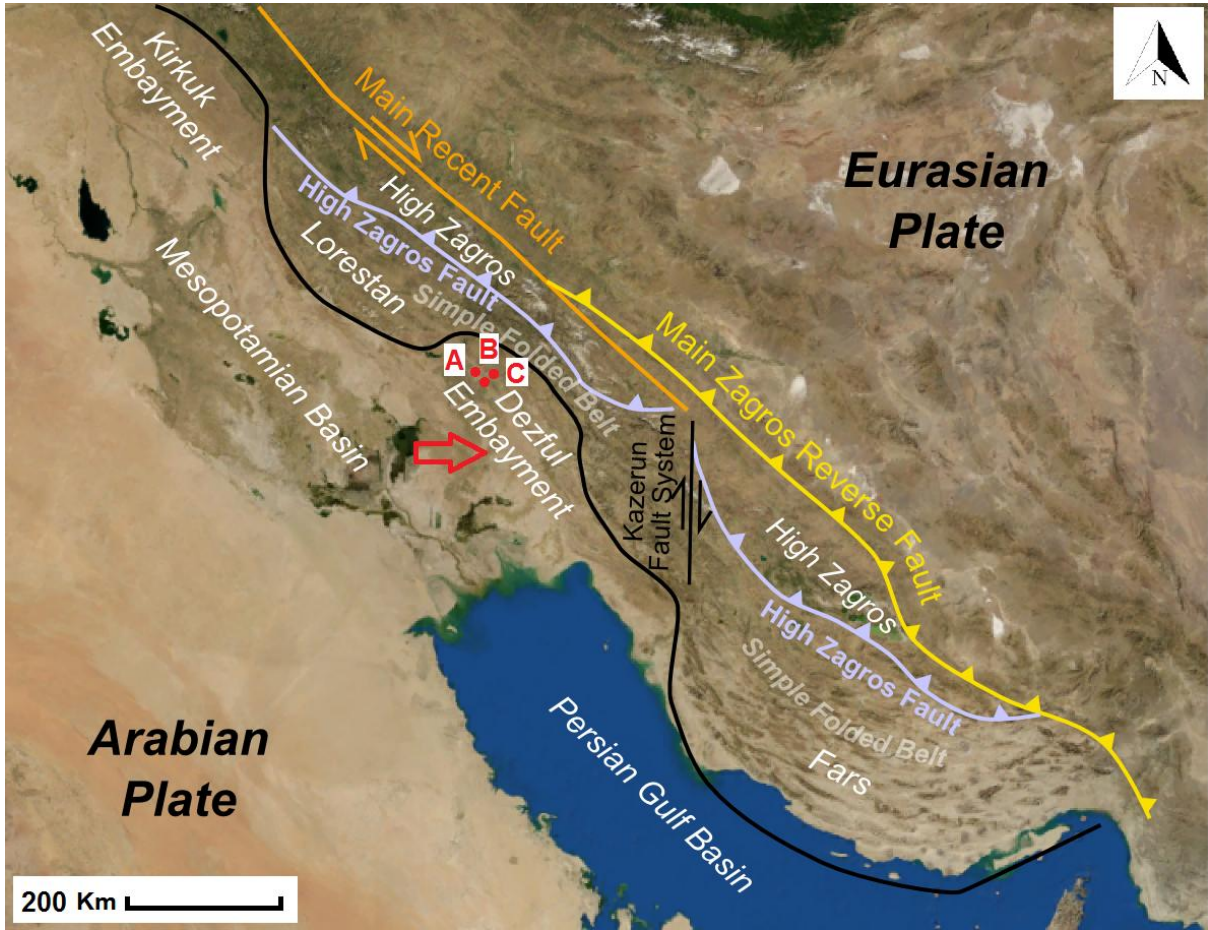


Fig. 1

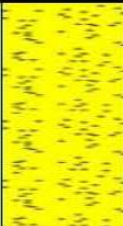




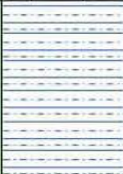


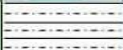


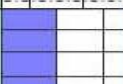
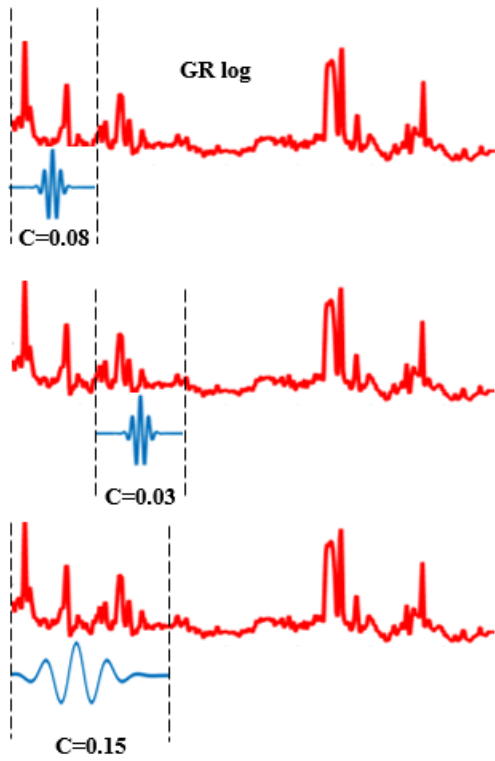
Formation		TOP (m)	Thickness (m)
Aghajari		Surface	1386
Mishan		1386	70
Gachsaran		1456	612
Asmari		2068	286
Pabdeh		2354	245
Gurpi		2599	294
Ilam		2893	203
Sarvak		3014	708
Kazhdumi		3722	260
Darian		3982	185
Gadvan		4167	167
Fahlian		4334	

Fig. 2

(a) Continuous Wavelet Transform



1. Choose a wavelet and compare it to a section at the start of the signal.
2. Calculate the correlation (C) between the wavelet and the chosen section of the signal. The larger the C number, the more the similarity.
3. Shift the wavelet to the right and repeat steps 1 and 2 until the whole signal is covered.
4. Stretch (scale) the wavelet and repeat the steps 1 through 3

(b) Discrete Wavelet Transform

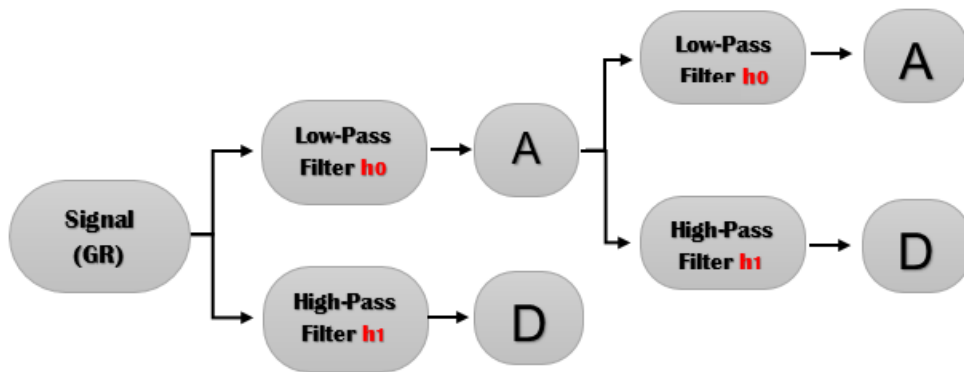


Fig. 3

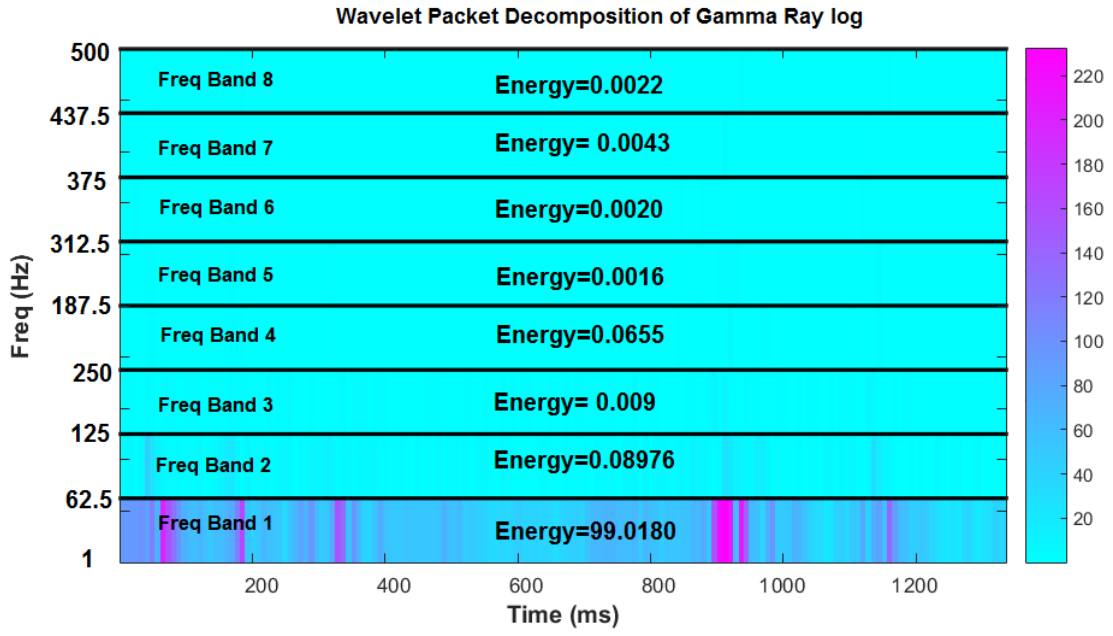


Fig. 4

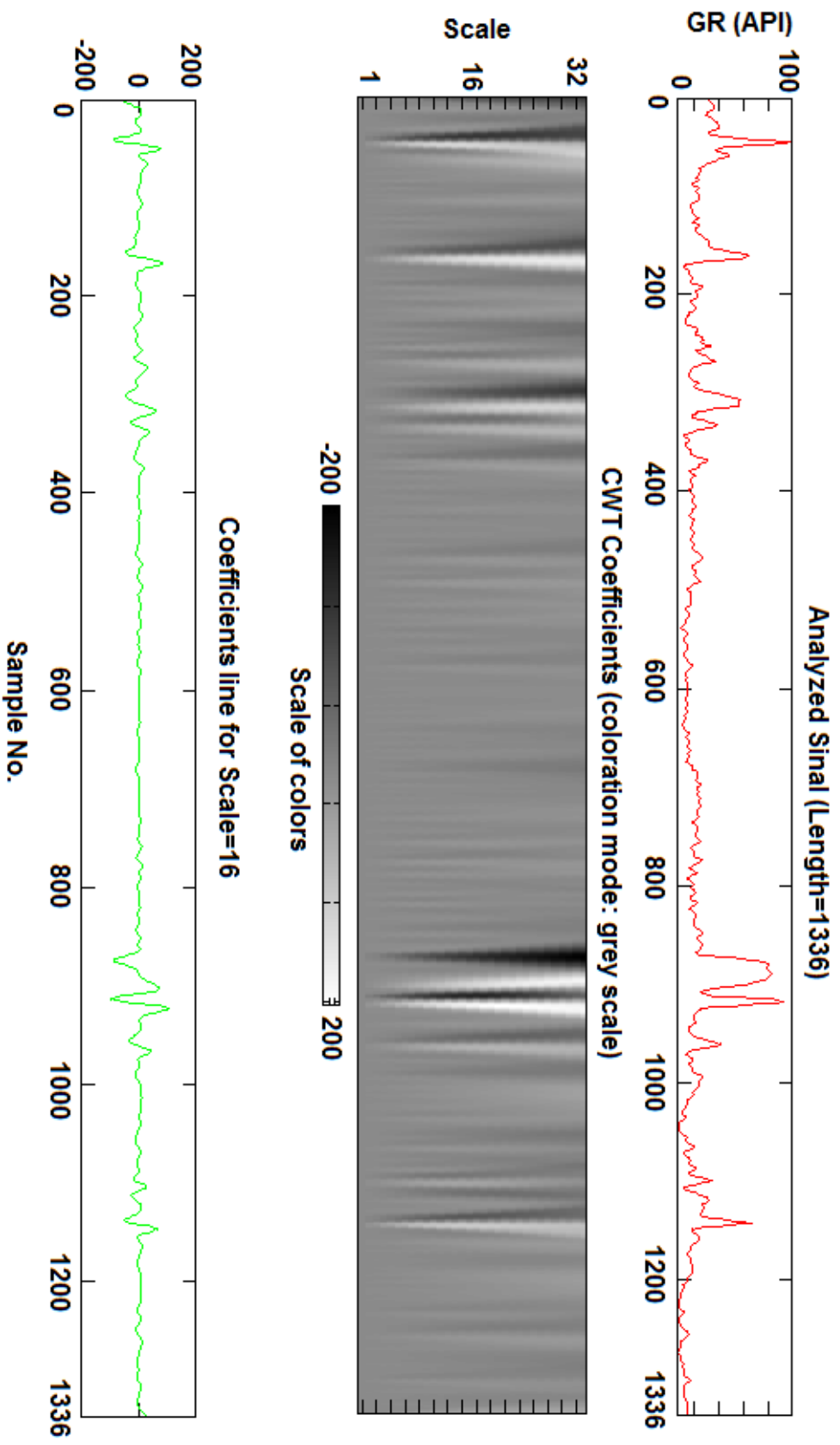


Fig. 5

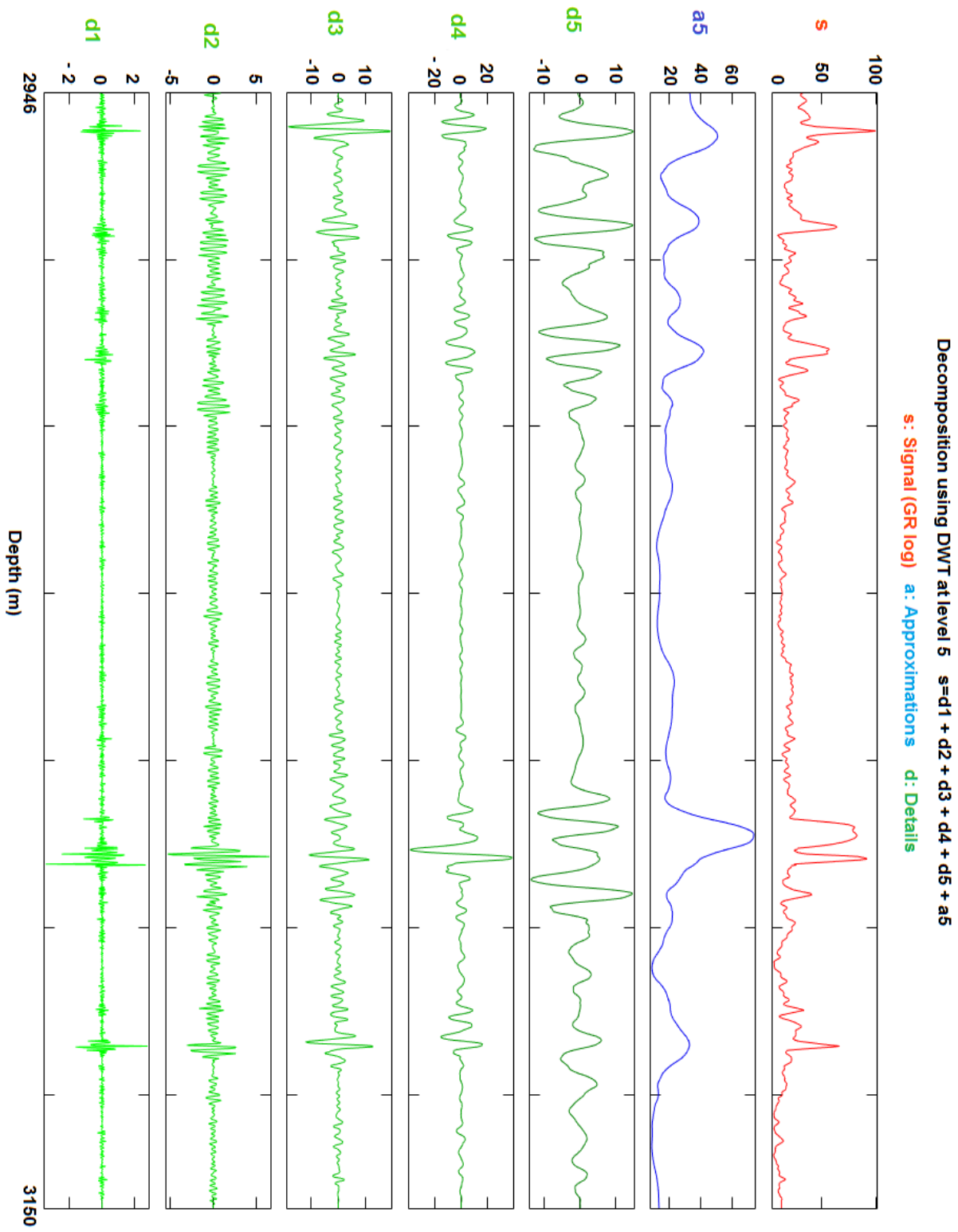


Fig. 6

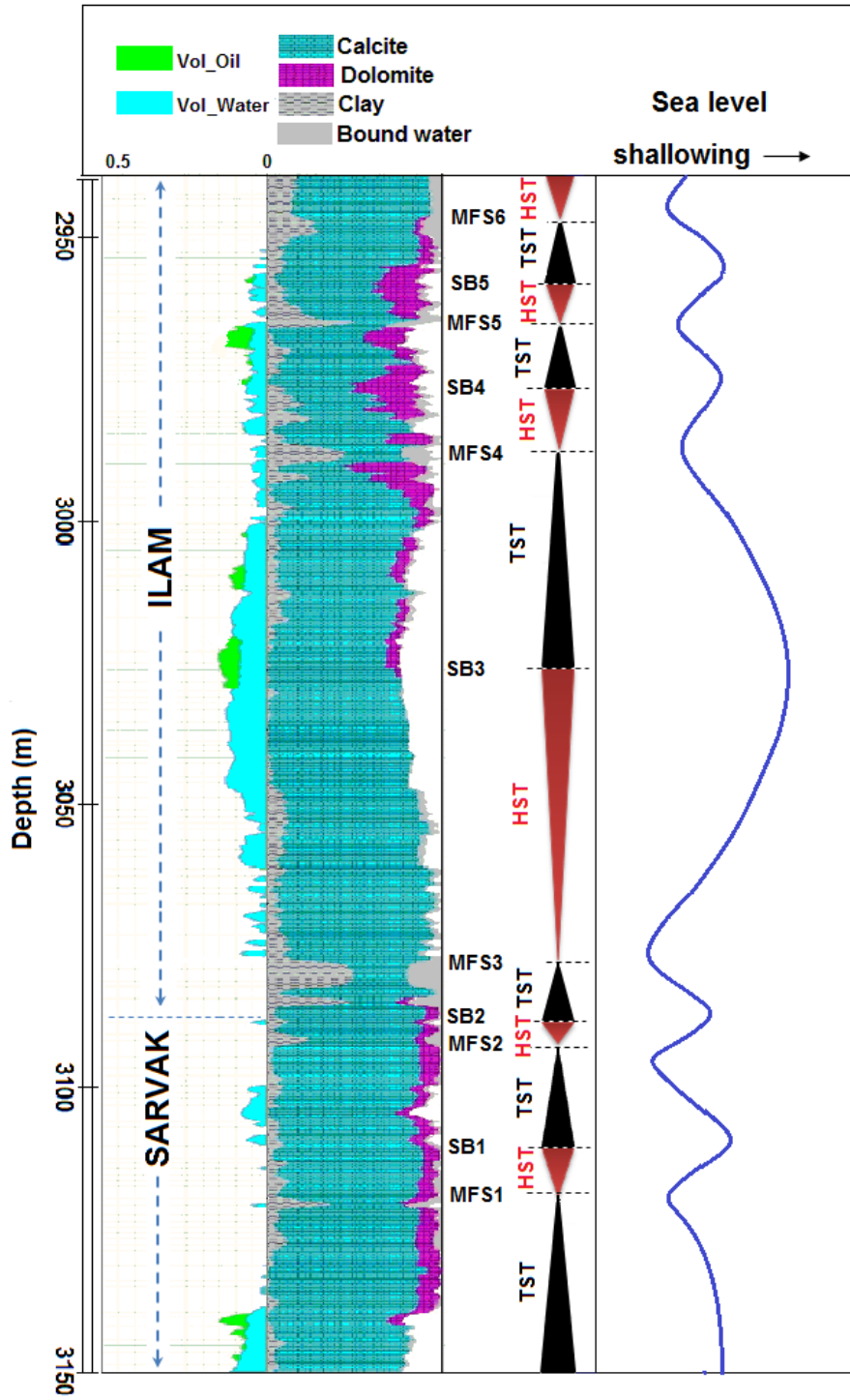


Fig. 7

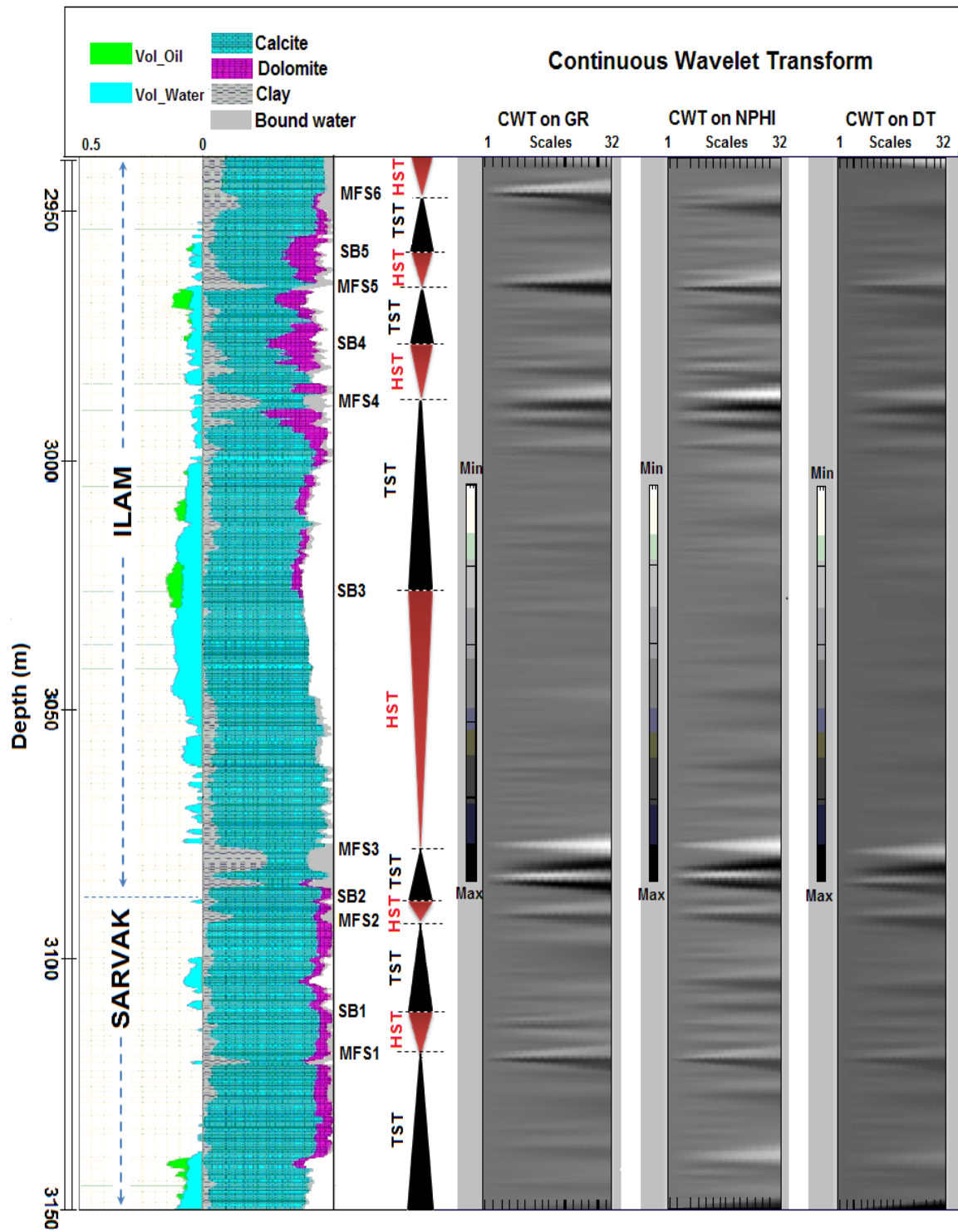


Fig. 8

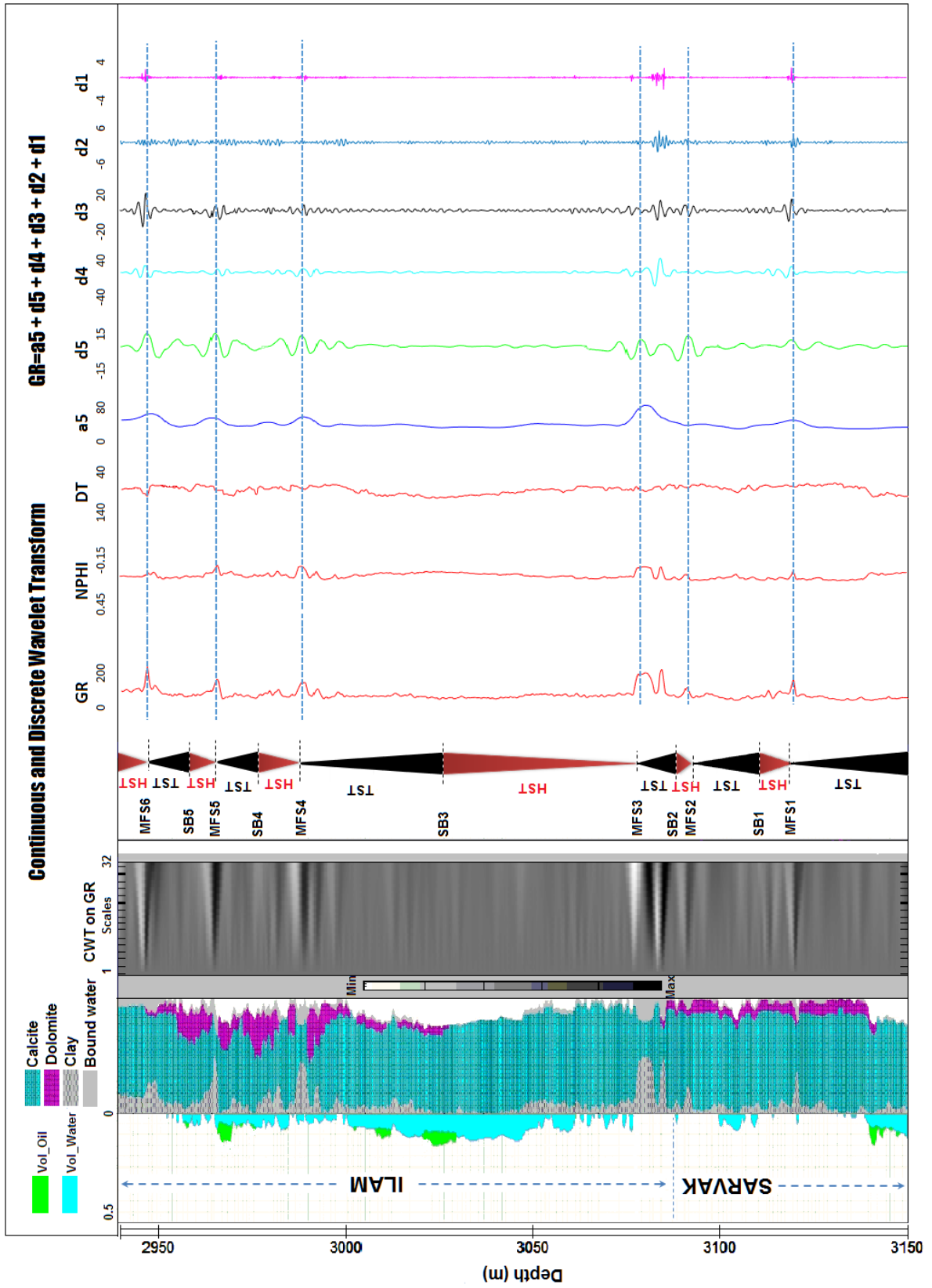


Fig. 9

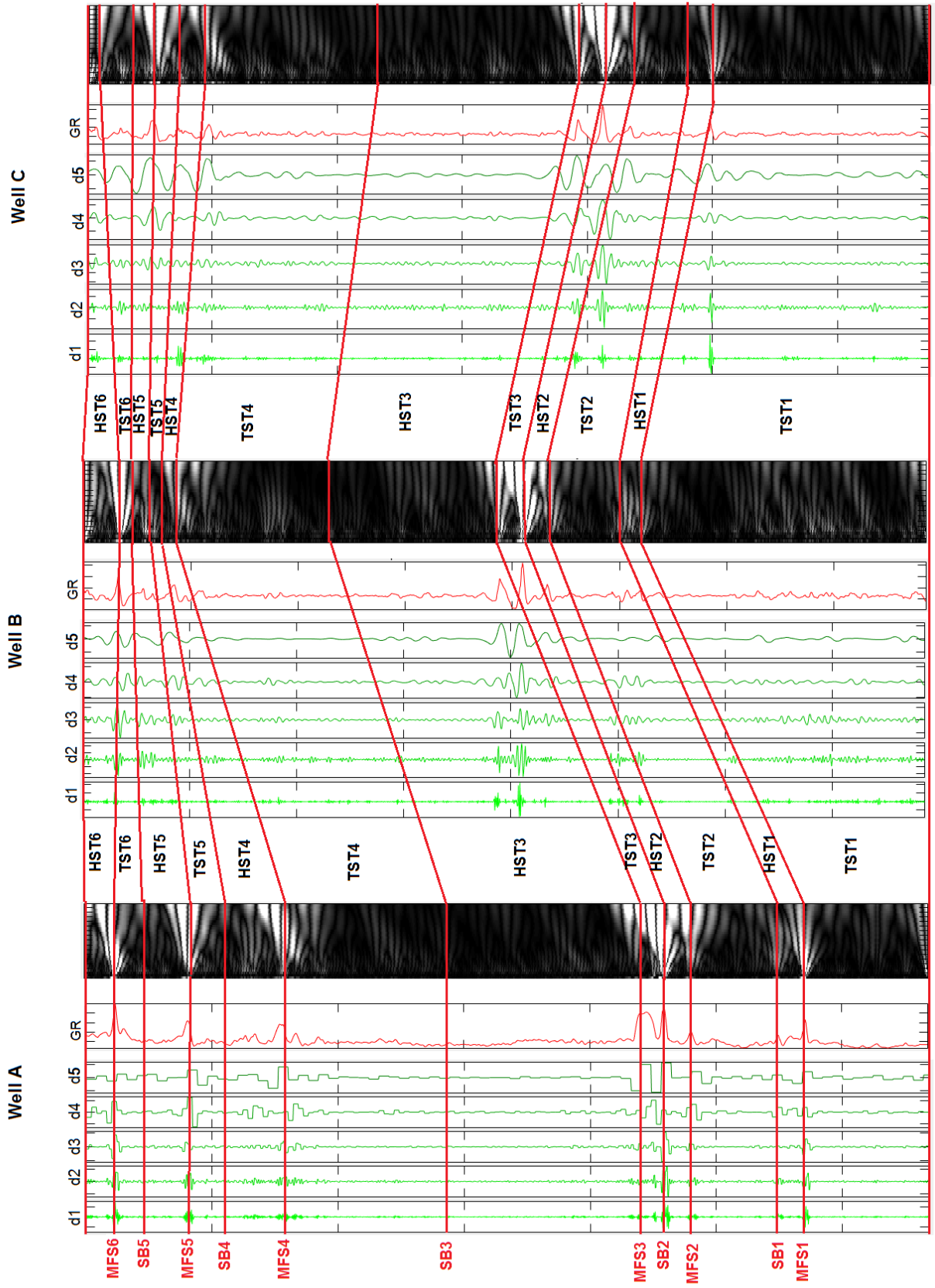


Fig. 10